# Experimental and Theoretical (DFT) Characterization of the Excited States and N-Centered Radical Species Derived from 2-Aminobenzimidazole, the Core Substructure of a Family of Bioactive Compounds

**Verónica Viudes,[†] Pavel Bartovský,[†] Luis R. Domingo,[‡] Rosa Tormos,*,[†] and Miguel A. Miranda*,[†]**

*Departamento de Química/Instituto de Tecnología Química UPV-CSIC, Universidad Politécnica de Valencia, Avenida de los Naranjos s/n, E-46022 Valencia, Spain, and Departamento de Química Orgánica, Universidad de Valencia, Dr. Moliner 50, E 46100 Burjassot, Valencia, Spain*

Fluorescence spectroscopy, laser flash photolysis (LFP), and density functional theory (DFT) calculations have been performed to understand the photobehavior of 2-aminobenzimidazole (**1**). The emission lifetime and quantum yield are solvent-dependent. Direct LFP of **1** at 266 nm in MeCN solution results in the generation of a transient identified as radical **1**(−H)• by comparison with the species generated upon *tert*-butyl peroxide (ROOR) irradiation in the presence of **1**. In addition, a transient assigned as the triplet state is detected in MeOH solution. Theoretical DFT studies on the hydrogen abstraction process support formation of a **1**···OR complex, which undergoes nitrogen to oxygen hydrogen transfer, producing the above-mentioned **1**(−H)• radicals.
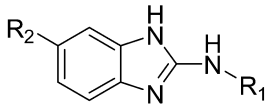
## Introduction

Benzimidazoles (BZs) have shown a broad spectrum of anthelmintic activity and are effective as antinematode and antiprotozoal agents.[1] In addition, many of them present antifungal activity and are used on fruits and vegetables.[2] In the last years the antitumoral behavior exhibited by many members of the family has attracted considerable attention.[3] In this context, the study of tubulin (TUB)−BZ interaction has been a very active area of research, in view of its biological importance. It seems accepted that BZs act by binding the $\beta$-TUB monomer before dimerization with $\alpha$-TUB with subsequent blockade of microtubule formation.[4] Recent efforts have been devoted to identify the binding domain of TUB,[5] and it has been proposed that BZs bind to a high-affinity site of the $\beta$-TUB monomer.[6]

To investigate the molecular basis of this behavior, photoaffinity labeling assays have been used, to identify the receptor and the ligand binding domain.[7] Likewise, analysis of BZ−$\beta$-TUB interaction has been performed using a fluorescence quenching methodology.[8] It is therefore surprising that little attention has been devoted to the effects of light on benzimidazoles. Thus, photochemistry studies are limited to the parent molecule and some of its alkyl derivatives,[9] although more recently the interest has been centered on the photoelimination of antifungal xenobiotics from the environment. For instance, the influence of UV light on the persistence of the most widely used benzimidazole carbamate fungicide, carbendazim, has been analyzed by different autors,[10] as this compound is toxic for humans and animals.

Specifically, 2-aminobenzimidazole (**1**) is the central building block of a number of bioactive benzimidazole derivatives (Chart 1). This moiety, highly fluorescent, is also present in the

**CHART 1: Structure of Some BZ Derivatives of Pharmaceutical Interest**



| Compound | $R_1$ | $R_2$ |
|---|---|---|
| 2-Aminobenzimidazole | H | H |
| Carbendazim | COOCH$_3$ | H |
| Mebendazole | COOCH$_3$ | Ph-CO- |
| Fenbendazole | COOCH$_3$ | Ph-S- |
| Oncodazole | COOCH$_3$ | Th-CO-[a] |

[a] Th = 2-thienyl.

structure of a variety of chemosensor receptors used for the selective recognition of anions with an important role in several biological activities, such as phosphate,[11] acetate,[12] iodide,[13] dicarboxylate,[14] etc. In spite of these applications, little is known on the photobehavior of **1**. The existing studies have focused on the effect of solvents and pH on the absorption and emission spectra; in addition, semiempirical molecular orbital calculations have been used as an approach to characterize the lowest singlet excited state.[15] However, the triplet excited state and other possible transients generated from **1** have not been investigated as of yet.

With this background, the aim of the present work is the full characterization of photophysical properties of 2-aminobenzimidazole. This knowledge is an essential requirement to check, in a later stage, the possibility of using **1** as a probe for tubulin-interaction studies through fluorescence and/or triplet excited state changes. In this context, it has recently been found that drug triplet excited states can be used as reporters for protein binding sites, as their lifetimes are markedly sensitive to the microenvironment experienced within these biomacromolecules.[16]

* Corresponding author. Fax: +34 963877809. E-mail address: mmiranda@qim.upv.es.
† Universidad Politécnica de Valencia.
‡ Universidad de Valencia.

## Experimental Section

**Materials and Solvents.** 2-Aminobenzimidazole, *S*-flurbiprofen, *tert*-butyl peroxide, and benzophenone were purchased from Aldrich. Their purity was checked by ^{1}H nuclear magnetic resonance (NMR) spectroscopy and high-performance liquid chromatography (HPLC) analysis.

The reagent grade solvents (acetonitrile and methanol) were purchased from Scharlau and used without further purification.

**Absorption Spectra.** Optical spectra in different solvents were measured on a Perkin-Elmer Lambda 35 UV/vis spectrophotometer.

**Fluorescence Measurements.** Emission spectra were recorded on a spectrofluorometer system, which was provided with an M 300 emission monochromator in the wavelength range of 200−900 nm and are uncorrected. Samples were placed into $10 \times 10$ mm[2] Suprasil quartz cells with a septum cap. Solutions were purged with nitrogen or oxygen for at least 10 min before the measurements. Fluorescence quantum yields were determined using *S*-flurbiprofen [*S*-2-fluoro-$\alpha$-methyl-4-biphenylacetic acid] as reference ($\Phi_F = 0.27$ at $\lambda_{exc} = 281$ nm in methanol as solvent).[17] The absorbance of the samples at the excitation wavelength was kept below 0.1. Excitation and emission slits were maintained unchanged during the emission experiments. For time-resolved fluorescence decay measurements, the conventional single photon counting was used. All experiments were performed at room temperature (22 °C).

**Laser Flash Photolysis Experiments.** The laser flash photolysis (LFP) experiments were carried out by using a Q-switched Nd:YAG laser (Quantel Brilliant, 266 or 355 nm, 10 or 14 mJ per pulse, 5 ns fwhm) coupled to an mLFP-111 Luzchem miniaturized equipment. This transient absorption spectrometer includes a ceramic xenon light source, 125 mm monochromator, Tektronix 9-bit digitizer TDS-3000 series with 300 MHz bandwidth, compact photomultiplier and power supply, cell holder and fiber optic connectors, fiber optic sensor for laser-sensing pretrigger signal, computer interfaces, and a software package developed in the LabVIEW environment from National Instruments. The LFP equipment supplies 5 V trigger pulses with programmable frequency and delay. The rise time of the detector/digitizer is approximately 3 ns up to 300 MHz (2.5 GHz sampling). The laser pulse is probed by a fiber that synchronizes the LFP system with the digitizer operating in the pretrigger mode. All transient spectra were recorded using $10 \times 10$ mm[2] quartz cells with 4 mL capacity, and some of them were bubbled during 20 min with $N_2$ or $O_2$ before acquisition. The absorbance of the samples was kept between 0.2 and 0.3 at the laser wavelength. All the experiments were carried out at room temperature.

**Computational Methods.** DFT calculations were carried out using the B3LYP[18] exchange-correlation functional together with the standard 6-31G(d) basis sets.[19] For the triplet and the radical species, the unrestricted formalism (UB3LYP) was employed. Optimizations were carried out using the Berny analytical gradient optimization method.[20] Vertical energies of the singlet-excited state were calculated using the time-dependent (TD-DFT) method[21] at the B3LYP/6-311+G(d,p) level. All calculations were carried out with the Gaussian 03 suite of programs.[22]

## Results and Discussion

**Absorption and Emission Properties of 2-Aminobenzimidazole.** As a preliminary stage, the absorption properties of 2-aminobenzimidazole were studied. As shown in Figure 1, the shape and position of the bands in aqueous solution are different
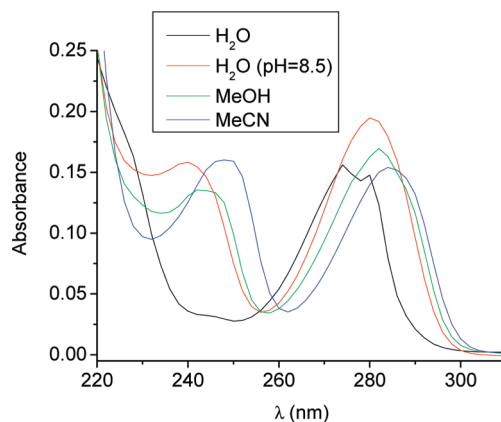


**Figure 1.** UV-absorption spectra of **1** in $H_2O$, MeCN, and MeOH ($1 \times 10^{-4}$ M) solutions.
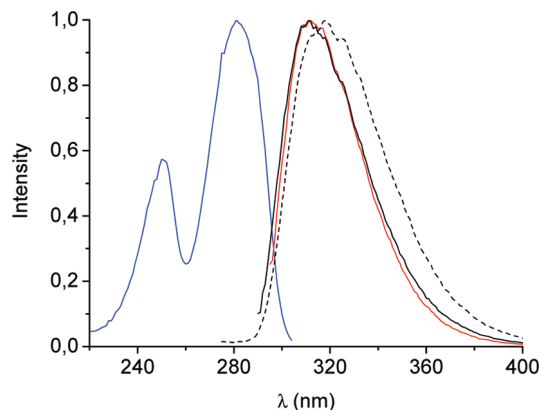


**Figure 2.** Normalized emission spectra of **1** in MeCN (red line), MeOH (black line), and $H_2O$ (pH = 8.5) (- - -) upon excitation at 280 nm, together with excitation spectrum in MeCN ($\lambda_{em} = 312$ nm).

from those obtained in organic solvents. Thus, the spectrum of **1** in water shows a band centered at 278 nm, while in MeOH or MeCN two bands appear with maxima at about 240 and 280 nm. This difference can be attributed to the basic character of **1** due to the guanidine-like moiety with three nitrogen atoms that are potential protonation sites. Depending on the pH value, compound **1** exists as the protonated or the neutral form. Thus, the spectrum obtained in water is assignable to the protonated form. Conversely, the neutral form is observed at pH ≥ 8.5 as indicated by the pH dependence of the **1** absorption spectrum (not shown).

Next, the emission spectra of **1** were recorded under different conditions, upon excitation at the long wavelength absorption band (280 nm). It was clearly observed (Figure 2) that the shape and position of the emission maximum in MeOH matched with that obtained in MeCN (312 nm), while in water it was shifted to 320 nm.

The excitation spectrum for the emission at 312 nm in MeCN solution is also shown in Figure 2. From the intersection between the two bands, after normalization, a singlet energy of 96 kcal/mol was determined. A similar value was obtained in the other solvents.

A summary of the photophysical properties of **1**, including fluorescence quantum yields and lifetimes under different conditions, is given in Table 1.

A significant difference was observed between the results obtained in organic and aqueous solution. Remarkably, in the latter medium the quantum yield was ca. 40 times lower than in MeCN or MeOH, and the lifetime (ca. 0.7 ns) was also

**6610**  *J. Phys. Chem. B, Vol. 114, No. 19, 2010*

Viudes et al.

**TABLE 1: Photophysical Properties of 2-Aminobenzimidazole[a]**

| solvent | $\Phi(N_2)$ | $\Phi(air)$ | $\tau(N_2)$ (ns) | $k_F$ (s$^{-1}$) |
|---|---|---|---|---|
| MeCN | 0.37 | 0.31 | 2.3 | $4.34 \times 10^8$ |
| MeOH | 0.45 | 0.35 | 2.7 | $3.70 \times 10^8$ |
| H$_2$O (pH = 8.5) | 0.01 | 0.01 | 0.6–0.8 | ca. $10^9$ |

[a] Data obtained upon excitation at 280 nm.
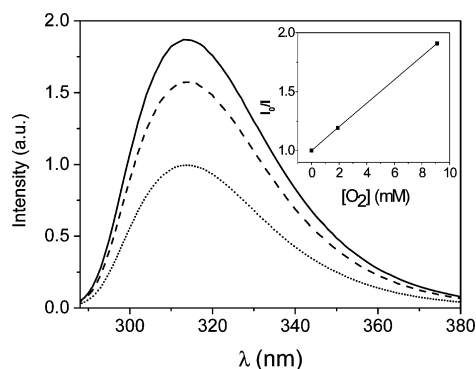


**Figure 3.** Emission spectra of **1** in MeCN under N$_2$ (—), air (- - -), and O$_2$ (· · ·). Inset: Stern−Volmer plot obtained for singlet quenching by O$_2$.

shorter. This is in agreement with previous observations[15] and can be attributed to a combination of faster deactivation by nonradiative pathways and enhanced photoionization leading to N-centered radicals (see below). Furthermore, the fluorescence of **1** was sensitive to the presence of oxygen (Figure 3). Thus, when the samples were purged with O$_2$ a decrease of the quantum yields was observed; for instance, in MeCN the values dropped from $\Phi = 0.37$ under inert atmosphere to $\Phi = 0.31$ in aerated solution and $\Phi = 0.19$ under oxygen.

From the Stern−Volmer plot (Figure 3, inset), a $k_q$ value of $4.3 \times 10^{10}$ M$^{-1}$ s$^{-1}$ was determined for **1** in MeCN solution using O$_2$ as quencher. In methanolic solution, $k_q$ resulted to be $3.4 \times 10^{10}$ M$^{-1}$ s$^{-1}$.

**Transient Absorption Spectroscopy of 2-Aminobenzimidazole.** After examining the absorption and emission behavior, transient absorption spectroscopy studies were undertaken. Thus, laser flash photolysis ($\lambda = 266$ nm) of a deaerated methanolic solution of **1** led to transients absorbing in the 275−520 nm range. The spectra obtained at short times after the laser pulses showed maxima at 340, 375, and 450 nm. However, after longer delay times, the signal peaking at 375 nm disappeared (see Figure 4A).

Figure 4B shows the transient absorption spectra upon 266 nm excitation of **1** in acetonitrile or water solution. The shape and position of the two obtained bands are very similar.

In principle, these signals could be assigned to radical cation, radical, and/or triplet formation. It is well-known that, due to their low oxidation potential, amines easily photoionize, giving a radical cation, whose deprotonation may afford a neutral radical. In addition, generation of the triplet excited state can also be expected.

To ascertain whether any of the transient absorption bands could be ascribed to the triplet, laser flash photolysis of aereated and deareated solutions of **1** in methanol was performed. Thus, the samples were excited at 266 nm, either bubbling N$_2$ or O$_2$. The difference spectrum showed a well-defined band centered at 375 nm that can be reasonably attributed to the T−T absorption of **1** (Figure 5). The triplet lifetime was determined to be 8.9 $\mu$s in methanolic solution.
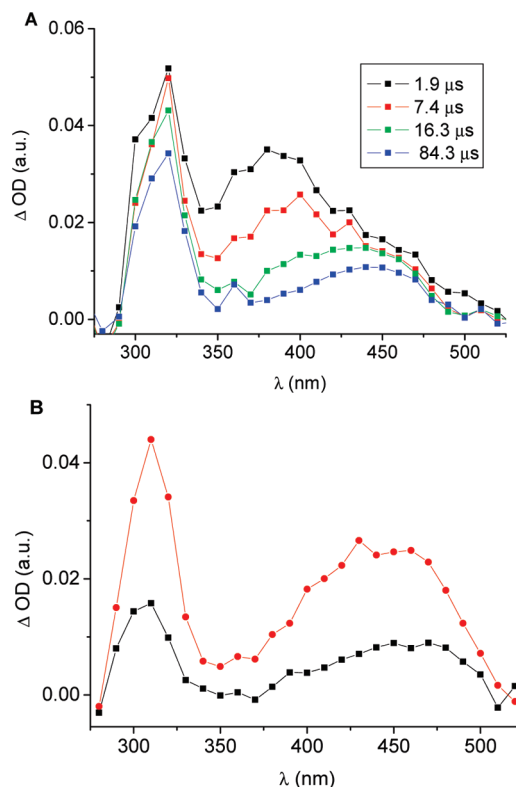


**Figure 4.** (A) Transient absorption spectra of 2-aminobenzimidazole ($4.5 \times 10^{-5}$ M) in MeOH after 266 nm irradiation at the indicated delay times. (B) Transient absorption spectra of 2-aminobenzimidazole ($4.5 \times 10^{-5}$ M) in MeCN (■) and aqueous solution (●) after 266 nm irradiation. The spectra were registered 1.1 $\mu$s after the laser pulse.
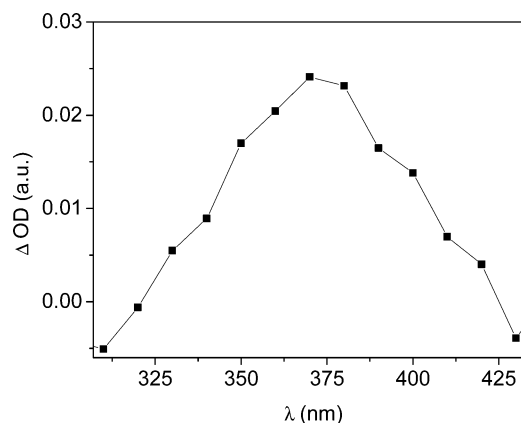


**Figure 5.** Spectrum resulting from subtraction of the traces obtained upon laser flash photolysis of **1** ($\lambda_{exc} = 266$ nm), in N$_2$ or O$_2$ bubbled methanolic solution.

To assign the band peaking at 450 nm as radical or radical cation, an alternative approach to generate the radical was used. Hence, a solution of **1** in a mixture of acetonitrile and *tert*-butyl peroxide (10:1, v/v) was irradiated at 355 nm. Under these conditions the generated *tert*-butoxy radical (RO$^•$) should abstract hydrogen from **1**, leading to formation of *tert*-butanol and an N-centered radical.[23] Figure 6 shows the resulting spectrum, and the inset displays the kinetics of its formation through the growth monitored at 450 nm. The recorded signal, although noisy, was similar to that obtained at 440 nm by direct irradiation of methanolic, acetonitrile, or aqueous solutions of **1**. Thus, it can be attributed to an N-centered radical.

In principle, formation of two radicals of this type is possible, depending on the hydrogen atom removed. Theoretical calcula-
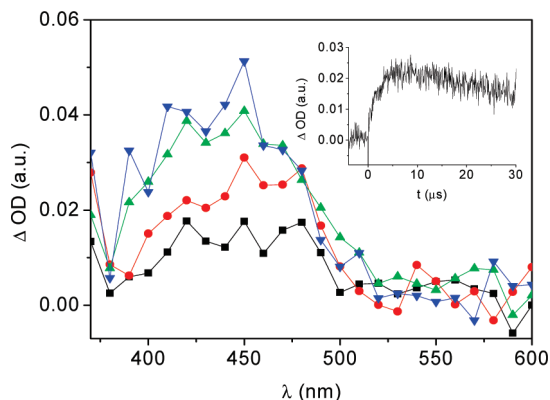
**Figure 6.** Transient absorption spectra obtained by 355 nm irradiation of a mixture of acetonitrile and *tert*-butylperoxide (10:1, v/v) in the presence of **1** ($10^{-3}$ M) registered at 0.26 $\mu$s (■), 1.28 $\mu$s (●), 3.24 $\mu$s (▲), and 6.47 $\mu$s (▼) after laser pulse. Inset: growth profile monitored at 440 nm.
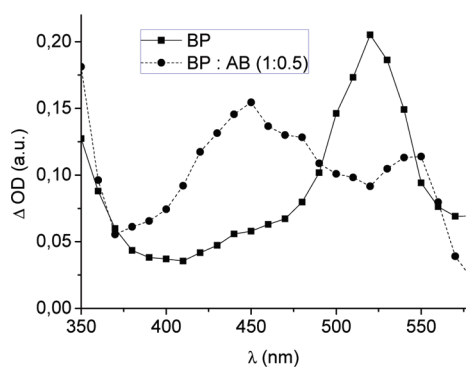


**Figure 7.** Transient absorption spectra obtained by 355 nm irradiation of $2 \times 10^{-3}$ M acetonitrile solutions of BP alone (■) and in the presence of **1** ($10^{-3}$ M) (●) registered 0.42 $\mu$s after the pulse.

tions (see below) demonstrated that hydrogen abstraction from the amino group is somewhat more favorable than from the NH group of the benzimidazole ring system.

Additional support in favor of radical formation was obtained by 355 nm laser flash photolysis of benzophenone (BP) in the presence of **1**, which led to a fast decay of the initially formed BP triplet signal at 525 nm, concomitant with the growth of two bands with maxima centered at 450 and at 550 nm (Figure 7).

Under these conditions, triplet—triplet energy transfer is not possible, as the triplet energy of benzophenone (69 kcal/mol) is lower than that of **1** (see calculations below). Thus, the transient bands can be safely assigned to the 2-aminobenzimidazole-derived radical (450 nm) and the well-known[24] ketyl radical (550 nm). Formation of these species can be explained through formal hydrogen abstraction from the amino group by the benzophenone triplet, either directly or by sequential electron—proton transfer.

The decay traces obtained for the radical generated by direct photolysis at 266 nm were satisfactorily fitted to monoexponential functions; the lifetime values in the used solvents were found to be 359.9 $\mu$s in MeOH, 299.1 $\mu$s in MeCN, and 258.8 $\mu$s in aqueous solution (pH = 8.5), respectively.

On the basis of absolute absorbance changes, and using BP in acetonitrile as actinometer, the $\varepsilon_{450}$ value for **1**$(-$H$)^\bullet$ was estimated at 14 040 $M^{-1}cm^{-1}$, whereas the quantum yield of radical formation was determined to be 0.11. Assuming that in MeOH and $H_2O$ the $\varepsilon$ values for this species are comparable, the formation quantum yields would be 0.13 and 0.30, respec-

**TABLE 2: (U)B3LYP/6-31G(d) Total (*E*, in au) and Relative (Δ*E*, in kcal/mol) Energies of the Stationary Points Involved in the Photoactivation/Deactivation of 1, Radicals R1, R2, and R3, and the Molecular Complexes MC1 and MC2**

|  | *E* | Δ*E* |
|---|---|---|
| **1** ($S_0$) | −435.226323 | |
| **1** ($S_1$) | −435.183053[a] | 105.4[a] |
| **1** ($T_{1v}$) | −435.083630 | 89.5 |
| **1** ($T_1$) | −435.099479 | 79.6 |
| **R1** | −434.585064 | 1.4 |
| **R2** | −434.587344 | 0.0 |
| **R3** | −434.578191 | 4.3 |
| *tert*-BuO$^\bullet$ | −233.006172 | |
| *tert*-BuOH | −233.670958 | |
| **MC1**a | −668.246103 | −8.5 |
| **MC1**b | −668.246153 | −8.6 |
| **MC2**-1 | −668.278841 | −29.1 |
| **MC2**a | −668.280039 | −29.8 |
| **MC2**b | −668.261597 | −18.3 |

[a] B3LYP/6-311+G(d,p) TD calculations (see text).

tively. The transient T−T absorption was only distinguishable in MeOH, where it always appeared together with other signals; hence, it was difficult to make accurate estimations on the intersystem crossing quantum yields. However, taking into account the efficiency of the competing processes, it was possible to set 0.4 as an upper limit for $\Phi_{isc}$ in all solvents.

**Theoretical DFT Calculations.** The structures of 2-aminobenzimidazole (**1**) at the singlet and triplet states were theoretically studied using density functional theory (DFT) methods at the B3LYP/6-31G(d) level. Excitation of **1** results in formation of the excited singlet state ($S_1$), which undergoes intersystem crossing (ISC) to the lower lying excited triplet state ($T_1$). Subsequent radiationless decay would lead back to the ground state ($S_0$). The B3LYP/6-311+G(d,p) time-dependent (TD) energy for vertical excitation of the chromophore to the singlet state $S_1$ was computed as 105.4 kcal/mol. At this level of calculations, **1** ($S_0$) would require absorption of 271.3 nm light ($f = 0.0047$) to reach $S_1$. The B3LYP/6-31G(d) vertical excitation of **1** ($S_0$) to the triplet state $T_1$ was found to be 89.5 kcal/mol. Relaxation of the triplet would result in a diminution of the $T_1$ energy down to 79.6 kcal/mol.

Upon interaction of **1** with the *tert*-butoxy radical, hydrogen donation can in principle lead to formation of *tert*-butanol and three feasible neutral radicals, depending on the nature of the removed hydrogen atom from **1** ($S_0$): N1−H (**R1**), amine−Ha (**R2**), or amine−Hb (**R3**).

The energies of **1** at the $S_0$, $S_1$, and $T_1$ states, as well as those of the corresponding neutral radical species, are given in Table 2, while the geometries of the radicals are shown in Figure 8.

Abstraction of the Ha hydrogen of the amine nitrogen atom leads to **R2**, the most stable radical species. On the other hand, **R1** and **R3** radicals, formed by abstraction of the hydrogens attached to the N1 nitrogen or the Hb hydrogen of the amine nitrogen, are 1.4 and 4.3 kcal/mol higher in energy, respectively. Since the *tert*-butoxy radical, as well as *tert*-butanol, can be hydrogen-bonded to **1** ($S_0$) or the neutral radicals, the corresponding molecular complexes **MC1** and **MC2** were optimized. The total and relative energies are also given in Table 2, while the geometries of the MCs are shown in Figure 9. The *tert*-butoxy radical can only form two different MCs because its oxygen atom is simultaneously hydrogen-bonded to the N−H and amine−Ha hydrogens, forming **MC1**a. Both **MC1**a and **MC1**b are more stable (8.5 and 8.6 kcal/mol, respectively) than
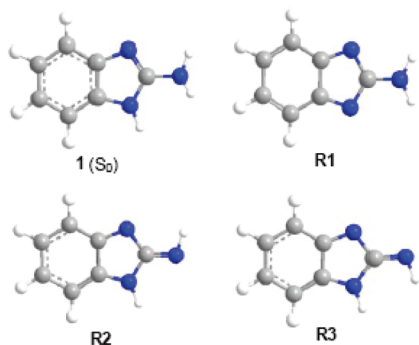
**Figure 8.** Geometry of the neutral radicals formed upon interaction between **1** and *tert*-butoxy radical.
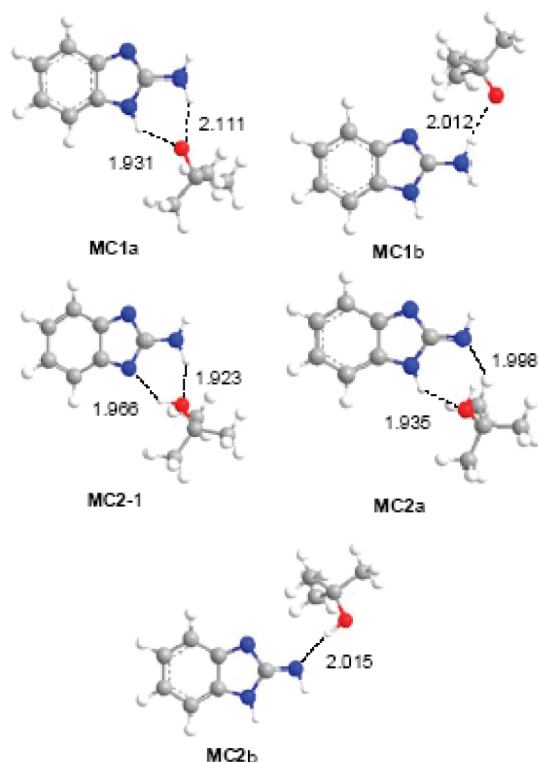


**Figure 9.** B3LYP/6-31G* structures of the molecular complexes. Distances are given in angstroms.

the separated reagents (**1** + **RO**·) as a consequence of hydrogen bond (HB) formation. After hydrogen donation from **1** to **RO**· at **MC1**a and **MC1**b, three new MCs can be formed. While **MC2**-1 and **MC2**a are 20.5 and 21.3 kcal/mol lower in energy than **MC1**a, **MC2**b is 9.7 kcal/mol more stable than **MC1**b. Consequently, these hydrogen abstractions are strongly exothermic and therefore thermodynamically favored. Note that after formation of the corresponding MCs the relative energy of **R1** decreases to 0.8 kcal/mol with respect to **R2**. On the other hand, formation of **MC2**b becomes thermodynamically disfavored with respect to **MC2**a by 11.6 kcal/mol. This is related to the fact that **MC2**a forms two HBs, whereas **MC2**b can only form one HB (see Figure 9).

Figure 8 shows the geometries of **1** ($S_0$) and the corresponding neutral radicals, **R1**, **R2**, and **R3**. The lengths of the N−H bonds at **1** ($S_0$) are 1.007 Å (N1−H), 1.011 Å (N−Ha), and 1.011 Å (N−Hb). While N−Ha is located near the plane of **1**, the N1−C2−N−Ha dihedral angle is 10° and the N−Hb is twisted −43°. This arrangement points to some pyramidalization of the amine N atom. The N1−H bond is somewhat twisted; 14°. For radical **R1**, the amine N−H bonds are 1.007 Å long, and both

of them are located on the molecular plane of **1**. This rearrangement points to a sp² hybridization of the amine nitrogen atom. For radical **R2**, the lengths of the N−H bonds are 1.008 Å (N1−H) and 1.020 Å (HN−H), whereas for radical **R3**, the lengths of the N−H bonds are 1.009 Å (N1−H) and 1.025 Å (HN−H). At **R2** and **R3**, both N−H bonds are positioned in the molecular plane. The C2−NH₂ bond lengths at these radicals are 1.338 (**R1**), 1.298 (**R2**), and 1.303 (**R2**) Å. Finally, at the MCs, the lengths of the HB are in the narrow range of 1.93 to 2.11 Å, indicating similar HB interactions.

## Conclusions

In summary, 2-aminobenzimidazole is a photoactive compound, which upon excitation gives rise to a variety of signals, potentially useful for the study of supramolecular interactions with proteins or other biomolecules. It can be promoted to a singlet excited state, with emission maxima at 312 nm, quantum yield of ca. 0.4, and lifetimes of ca. 2.5 ns. The fluorescence properties are medium sensitive; in aqueous environment and/ or under aerobic atmosphere, both the emission intensities and lifetimes experience a marked decrease. Transient absorption spectroscopy reveals formation of a detectable triplet excited state peaking at 375 nm, as well as a N-centered radical appearing at 450 nm. The relative contributions of these species to the overall spectrum also depend on the nature of the employed solvent, thus the triplet is more clearly observable in methanolic solution. Theoretical DFT calculations have provided a reasonable estimation of the excited state energies and rationalize formation of the N-centered radical, supporting its assignment as resulting through formal H-abstraction from the exocyclic amino group.

## References and Notes

(1) (a) Behnke, J. M.; Buttle, D. J.; Stepek, G.; Lowe, A.; Duce, I. R. *Parasites Vectors* **2008**, 1. (b) Prichard, R. K. *Parasitology* **2007**, *134*, 1087. (c) Prichard, R. K.; von Samson-Himmelstjerna, G.; Blackhall, W. J.; Geary, T. G. *Parasitology* **2007**, *134*, 1073. (d) von Samson-Himmelstjerna, G.; Blackhall, W. J.; McCarthy, J. S.; Skuce, P. J. *Parasitology* **2007**, *134*, 1077. (e) Bossche van de, M.; Thienpoint, D.; Janssens, P. G. *Chemotherapy of gastrointestinal Helminths*; Springer: Berlin, 1985. (f) Reynoldson, J. A.; Thompson, R. C. A.; Meloni, B. P. *Biochem. Protozol.* **1991**, *52*, 587.

(2) (a) Das, H.; Jayaraman, S.; Naika, M.; Bawa, A. S. *J. Food Sci. Technol.* **2007**, *44*, 587. (b) Tahara, S.; Ingham, J. L. *Stud. Nat. Prod. Chem.* **2000**, *22*, 457. (c) Davidse, L. C. *Annu. Rev. Phytopathol.* **1986**, *24*, 43–65.

(3) (a) Steams, M. E.; Wang, M.; Fudge, K. *Cancer Res.* **1993**, *53*, 3073. (b) Boiani, M.; Gonzalez, M. *Min. Rev. Med. Chem.* **2005**, *5*, 409. (c) Wang, X.; Cheung, H. W.; Chun, A. C S; Jin, D.; Wong, Y. *Front. Biosci.* **2008**, *13*, 2013. (d) Meng, L.; Liao, Z.; Pommier, Y. *Curr Top. Med. Chem.* **2003**, *3*, 305. (e) Clement, M. J.; Rathinasamy, K.; Adjadj, E.; Toma, Flavio, C.; Patrick, A.; Panda, D *Biochemistry* **2008**, *47*, 13016.

(4) Kwa, M. S.; Veenstra, J. G.; Van Dijk, M.; Roos, M. H. *J. Mol. Biol.* **1995**, *246*, 500.

(5) (a) von Samson-Himmelstjerna, G.; Blackhall, W. J.; McCarthy, J. S.; Skuce, P. *J. Parasitol.* **2007**, *134*, 1077. (b) Didier, E. S.; Maddry, J. A.; Brindley, P. J.; Stovall, M. E.; Didier, P. J. *Expert Rev. Anti-Infect. Ther.* **2005**, *3*, 419. (c) Hoeglund, J.; Gustafsson, K.; Ljungstroem, B-L; Engstroem, A.; Donnan, A.; Skuce, P. *Vet. Parasitol.* **2009**, *161*, 60. (d) Clement, M-J; Rathinasamy, K.; Adjadj, E.; Toma, F.; Curmi, P. A.; Panda, D. *Biochemistry* **2008**, *47*, 13016.

(6) Lubega, G. W.; Geary, T. G.; Klein, R. D.; Prichard, R. K. *Mol. Biochem. Parasitol.* **1993**, *62*, 281.

(7) (a) Nare, B.; Liu, Z.; Prichard, R. K.; Georges, E. *Biochem. Pharmacol.* **1994**, *48*, 2215. (b) Nare, B.; Lubegas, G.; Prichard, R. K.; Georges, E. *J. Biol. Chem.* **1996**, *271*, 8575.

Core Substructure of a Family of Bioactive Compounds

*J. Phys. Chem. B, Vol. 114, No. 19, 2010* **6613**

(8) MacDonald, L. M.; Armson, A.; Thompson, R. C. A.; Reynoldson, J. A. *Mol. Biochem. Parasitol.* **2004**, *138*, 89.

(9) Cole, E. R.; Crank, G.; Lye, E. *Aust. J. Chem.* **1978**, *31*, 2675. (b) Crank, G.; Mursyldi, A. *Aust. J. Chem.* **1982**, *35*, 775.

(10) (a) Mazellier, P.; Leroy, E.; Legube, B. *J. Photochem. Photobiol., A: Chem.* **2002**, *153*, 221. (b) Boudina, A.; Emmelin, C.; Baaliouamer, A.; Grenier-Loustalot, M. F.; Cjovelon, J. M. *Chemosphere* **2002**, *5*, 649. (c) Escalada, J. P.; Pajares, A.; Gianotti, J.; Massad, W. A.; Bertolotti, S.; Amat-Guerri, F.; Garcia, N. A. *Chemosphere* **2006**, *65*, 237.

(11) Lee, G. W.; Singh, N.; Jang, D. O. *Tetrahedron Lett.* **2008**, *49*, 1952.

(12) (a) Joo, T. Y.; Singh, N.; Lee, G. W.; Jang, D. O. *Tetrahedron Lett.* **2007**, *48*, 8846.

(13) Singh, N.; Jang, D. O. *Org. Lett.* **2007**, *9*, 1991.

(14) Kim, H. S.; Moon, K. S.; Jang, D. O. *Supramol. Chem.* **2006**, *18*, 97.

(15) (a) Behera, P. K.; Mishra, H. P. *Indian J. Chem.* **1993**, *32A*, 418. (b) Mishra, A. K.; Dogra, S. K. *Indian J. Chem.* **1985**, *24A*, 815.

(16) (a) Jiménez, M C.; Miranda, M. A.; Vayá, I. *J. Am. Chem. Soc.* **2005**, *127*, 10134. (b) Lhiaubet-Vallet, V.; Sarabia, Z.; Bosca, F.; Miranda, M. A. *J. Am. Chem. Soc.* **2004**, *126*, 9538. (c) Lhiaubet-Vallet, V.; Bosca, F.; Miranda, M. A. *J. Phys. Chem. B* **2007**, *111*, 423. (d) Vayá, I.; Bueno, C. J.; Jiménez, M. C.; Miranda, M. A. *Chem.−Eur. J.* **2008**, *14*, 11284.

(17) Jiménez, M. C.; Miranda, M. A.; Tormos, R.; Vayá, I. *Photochem. Photobiol. Sci.* **2004**, *3*, 1038.

(18) (a) Lee, C.; Yang, W.; Parr, R. G. *Phys. Rev. B* **1998**, *37*, 785. (b) Becke, A. D. *J. Chem. Phys.* **1993**, *98*, 5648.

(19) Hehnre, W. J.; Radom, L.; Schleyer, P. V. R.; Pople, J. A. *Ab initio Molecular Orbital Theory*; Wiley: New York, 1986.

(20) (a) Schlegel, H. B. *J. Comput. Chem.* **1982**, *3*, 214. (b) Schlegel, H. B. *Geometry Optimization on Potential Energy Surface," in Modern Electronic Structure Theory*; Yarkony, D. R., Ed.; World Scientific Publishing: Singapore, 1994.

(21) (a) Bauernschmitt, R.; Ahlrichs, R. *Chem. Phys. Lett.* **1996**, *256*, 454–464. (b) Casida, M. E.; Jamorski, C.; Casida, K. C.; Salahud, D. R. *J. Chem. Phys.* **1998**, *108*, 4439.

(22) Frisch, M. J.; Trucks, G. W.; Schlegel, H. B.; Scuseria, G. E.; Robb, M. A.; Cheeseman, J. R.; Montgomery, J. A., Jr.; Vreven, T.; Kudin, K. N.; Burant, J. C.; Millam, J. M.; Iyengar, S. S.; Tomasi, J.; Barone, V.; Mennucci, B.; Cossi, M.; Scalmani, G.; Rega, N.; Petersson, G. A.; Nakatsuji, H.; Hada, M.; Ehara, M.; Toyota, K.; Fukuda, R.; Hasegawa, J.; Ishida, M.; Nakajima, T.; Honda, Y.; Kitao, O.; Nakai, H.; Klene, M.; Li, X.; Knox, J. E.; Hratchian, H. P.; Cross, J. B.; Adamo, C.; Jaramillo, J.; Gomperts, R.; Stratmann, R. E.; Yazyev, O.; Austin, A. J. ; Cammi, R.; Pomelli, C.; Ochterski, J. W.; Ayala, P. Y.; Morokuma, K.; Voth, G. A.; Salvador, P.; Dannenberg, J. J.; Zakrzewski, V. G.; Dapprich, S.; Daniels, A. D.; Strain, M. C.; Farkas, O.; Malick, D. K.; Rabuck, A. D.; Raghavachari, K.; Foresman, J. B.; Ortiz, J. V.; Cui, Q.; Baboul, A. G.; Clifford, S.; Cioslowski, J.; Stefanov, B. B.; Liu, G.; Liashenko, A.; Piskorz, P.; Komaromi, I.; Martin, R. L.; Fox, D. J.; Keith, T.; Al-Laham, M. A.; Peng, C. Y.; Nanayakkara, A.; Challacombe, M.; Gill, P. M. W.; Johnson, B.; Chen, W.; Wong, M. W.; Gonzalez, C.; Pople, J. A. *Gaussian 03*, revision C.02; Gaussian, Inc.: Wallingford, CT, 2004.

(23) Paul, H.; Small, R. D.; Scaiano, J. C. *J. Am. Chem. Soc.* **1978**, *100*, 4520.

(24) Sakaguchi, Y.; Hayashi, H.; Nagakura, S. *J. Phys. Chem.* **1982**, *86*, 3177.